

## Comparison of CD38 targeted alpha- vs beta-radionuclide therapy of disseminated multiple myeloma in an animal model

Megan Minnix<sup>1,2\*</sup>, Vikram Adhikarla<sup>3\*</sup>, Enrico Caserta<sup>4\*</sup>, Erasmus Poku<sup>5</sup>, Russell Rockne<sup>3</sup>, John E. Shively<sup>1\*\*</sup> and Flavia Pichiorri<sup>4\*\*</sup>

<sup>1</sup>Department of Molecular Imaging and Therapy, Beckman Research Institute, City of Hope, Duarte, CA, 91010.

<sup>2</sup>Irell and Manella Graduate School of Biological Sciences, Beckman Research Institute, City of Hope, Duarte, CA, 91010.

<sup>3</sup>Department of Computational and Quantitative Medicine, Division of Mathematical Oncology, Beckman Research Institute, City of Hope, Duarte, CA, 91010.

<sup>4</sup>Department of Hematologic Malignancies Research Institute, City of Hope Medical Center, Duarte CA 91010.

<sup>5</sup>Radiopharmacy, City of Hope Medical Center, Duarte CA 91010.

\*These authors contributed equally to this research.

\*\*To whom to address correspondence, City of Hope, 1550 East Duarte Rd, Duarte CA 91010, email: [jshively@coh.org](mailto:jshively@coh.org), [fpichiorri@coh.org](mailto:fpichiorri@coh.org); phone: 626-301-8308, fax: 626-301-8167

Running title:  $\alpha$ - vs  $\beta$ -radioimmunotherapy in multiple myeloma

Word count: 4194

Author contributions: MM designed, carried out the in vivo studies, analyzed data, wrote the first draft; VA performed the mathematical modeling; EC assisted in the therapy studies; EP performed the radiolabeling; RR, JES and FP supervised the study and edited the manuscript.

## ABSTRACT

Targeted therapies for multiple myeloma (MM) include the anti-CD38 antibody daratumumab (Dara), which, in addition to its inherent cytotoxicity, can be radiolabeled with tracers for imaging and with  $\beta$ - and  $\alpha$ -emitter radionuclides for radioimmunotherapy. **Methods:** We have compared the potential therapeutic efficacy of  $\beta$ -vs  $\alpha$ -emitter radioimmunotherapy using radiolabeled DOTA-Dara in a preclinical model of disseminated MM. Multiple dose levels were investigated to find the dose with the highest efficacy and lowest toxicity. **Results:** In a dose-response study with the  $\beta$ -emitter  $^{177}\text{Lu}$ -DOTA-Dara, the lowest tested dose of 1.85 MBq extended survival from 37 to 47d, but had no delay of tumor growth. The doses of 3.7 and 7.4 MBq extended survival to 55 and 58d, respectively, causing a small equivalent delay of tumor growth, followed by regrowth. The higher dose of 11.1 MBq eradicated the tumor but had no effect on survival compared to untreated controls, because of whole-body toxicity. In contrast, there was a dose-dependent effect of the  $\alpha$ -emitter  $^{225}\text{Ac}$ -DOTA-Dara, in which 0.925, 1.85, and 3.7 kBq increased survival, compared to untreated controls (35d), to 47d, 52d, and 73d, respectively, with a significant delay of tumor growth for all three doses. Higher doses of 11.1 and 22.2 kBq resulted in equivalent survival to 82d but with significant whole-body toxicity. Parallel studies with untargeted  $^{225}\text{Ac}$ -DOTA-trastuzumab conferred no improvement over untreated controls and resulted in whole-body toxicity. **Conclusion:** We conclude, and mathematical modeling confirms, that maximal biological doses were achieved by targeted alpha therapy and demonstrated  $^{225}\text{Ac}$  to be superior to  $^{177}\text{Lu}$  in delaying tumor growth and decreasing whole body toxicity.

Key words: CD38, daratumumab, multiple myeloma, radioimmunotherapy, mathematical modeling

## INTRODUCTION

Multiple myeloma (MM) is a malignancy of fully differentiated plasma cells that is normally confined to the bone marrow compartment, although extramedullary malignancies are often observed. Approximately 30,000 new cases of MM occur, with over 12,000 deaths, per year (1). Daratumumab (Dara) is a humanized anti-CD38 IgG<sub>1</sub> antibody against the surface receptor CD38, which is highly expressed on MM plasma cells but also on NK cells and monocytes in MM patients. Dara, either as a single agent or in combination with other agents, has yielded substantially favorable outcomes. Given the especially strong efficacy afforded by Dara with immunomodulatory drugs (IMiDs, lenalidomide and pomalidomide) (2-6), Dara+IMiDs are now FDA approved for advanced relapsed MM (2). The main anti-MM effect of Dara has thus far been attributed to its ability to target the MM cells via the immune system (7), but unfortunately a subset of patients do not respond to the treatment, while others may experience disease progression within a few months. Even in patients experiencing a long-lasting response, resistance eventually occurs. Although CD38 is highly expressed in MM, patient response to this therapy is variable, with some patients developing resistance in spite of continued high expression of the CD38 antigen on MM cells (8), supporting that antigen loss is not necessarily a consideration in the design of Dara-based therapies, as we recently published (9).

Since CD38 is ubiquitously expressed on the myeloma cells independently of the line of therapy, and Dara is able to directly target myeloma cells in the bone marrow (10,11), it is anticipated that addition of a therapeutic agent, such as a radionuclide, to Dara would dramatically increase its potency compared to the antibody alone, especially in patients who are progressing under regimens containing Dara. In this respect, several groups have explored the use of  $\alpha$ - and  $\beta$ -emitting radionuclides conjugated to anti-CD38 antibodies for improved therapy. Kang et al. showed that a DTPA-based chelate conjugate of Dara labeled with <sup>177</sup>Lu, a  $\beta$ -emitter with a tissue path length of about 2 mm, reduced tumor growth in a subcutaneous model of MM (12). Although  $\beta$ -emitter radionuclides have enjoyed some success in the treatment of disseminated diseases such as leukemia and lymphoma, they suffer from extensive

bone marrow suppression, often the rate limiting toxicity (13). Recently, investigators have become interested in  $\alpha$ -emitter radionuclides because of their shorter tissue path lengths (50-80  $\mu\text{m}$ , several cell diameters) and high linear energy transfer (LET) (14,15). In this regard, several  $\alpha$ -emitters, including  $^{213}\text{Bi}$ ,  $^{212}\text{Pb}$  and  $^{225}\text{Ac}$ , have been evaluated for targeting CD38 in multiple myeloma models (16-18). Each of these alpha emitters differ in their radiological half-lives, with implications for their suitability for therapeutic studies, since the anti-CD38 antibody biological half-life may be measured in weeks (19). With this consideration in mind, the 10-day radiological half-life of  $^{225}\text{Ac}$ , plus its decay scheme delivering 4 alpha particles over its half-life, is especially attractive. Accordingly, in a subcutaneous model of MM treated with  $^{225}\text{Ac}$ -labeled Dara, Dawicki *et al.* showed decreased tumor growth rate in treated versus the control groups (18).

In this study, we compared Dara labeled with the  $\beta$ -emitter  $^{177}\text{Lu}$  to that labeled with the  $\alpha$ -emitter  $^{225}\text{Ac}$  in a disseminated model of MM, and on the basis of these data, we performed mathematical modeling as a tool for quantifying the radiobiological effect for future applications of dose optimization.

## **MATERIALS AND METHODS**

### **Antibodies, Reagents and Cell Lines**

Daratumumab, anti-CD38 antibody, was obtained from Janssen Biotech Inc. (Titusville, NJ). GFP-Luciferase positive (Gfp/Luc) MM1-S MM cells were provided by Dr. Irene Ghobrial (Dana-Farber Cancer Institute, Boston, MA). 1,4,7,10-Tetraazacyclododecane-1,4,7,10-tetraacetic acid mono-N-hydroxysuccinimide ester (DOTA-NHS-ester) was from Macrocyclics, Inc., Plano, TX.  $^{225}\text{Ac}$  and  $^{177}\text{Lu}$  were obtained from the Department of Energy, Oakridge National Laboratory, Oakridge, TN.

### **Animal Studies and Bioluminescence Imaging**

All animal studies were performed in NOD.Cg-Prkdc<sup>scid</sup> Il2rg<sup>tm1Wjl</sup>/SzJ mice (NSG; 6-10 weeks old; Jackson Laboratory) in accordance with IACUC protocol 14043 approved by the City of Hope Institutional Animal Care and Use Committee, and in

accordance with the NIH Office of Laboratory Animal Welfare guidelines. Animals were housed in pie cages, in a specific pathogen free (SPF) room, with a maximum of 5 mice per cage. The MM1-S cell line was injected intravenously (IV), at  $5 \times 10^6$  cells/200  $\mu$ L PBS per mouse. Tumor distribution and growth was followed by serial whole-body imaging on the Lago X (Spectral Instruments Imaging, Tucson, AZ). Before in vivo imaging, animals were anesthetized with 4% isoflurane and injected intraperitoneally with 200  $\mu$ L D-luciferin (15 mg/ml) in sterile PBS. All bioluminescence imaging (BLI) data are depicted in radiance units (photons/s/cm<sup>2</sup>/sr) measured over the whole body as the region of interest. Mice were grouped so that the average BLI was similar across all groups. Whole body toxicity was measured by monitoring weight loss over time, with weight loss >20% considered an experimental endpoint. Paralysis of the mouse hind legs, a common symptom of the MM tumor models, was used as an alternative endpoint.

## **Radiolabeling**

Dara or control trastuzumab (Tras) antibodies were reacted with a 30 molar excess of the chelator DOTA-NHS ester as previously described (20). DOTA conjugation was confirmed by Q-TOF mass spectrometry (Agilent Technology 6510 QTOF LC/MS) as follows: 6  $\mu$ g of antibody was reduced with 1  $\mu$ L of 0.2 M Tris(2-carboxyethyl)phosphine (TCEP) for 2 hours at 37°C and then analyzed on an HPLC protein Agilent chip (Agilent Technologies, Santa Clara, CA). DOTA-conjugated antibody (200  $\mu$ g) was incubated with <sup>177</sup>Lu at a labeling ratio of 0.37 MBq/ $\mu$ g for 45 min at 43°C, chased with 1 mM diethylenetriamine pentaacetic acid (DTPA), and purified on a size-exclusion, preparative column (Superdex-200; GE Healthcare Life Sciences). DOTA-conjugated antibody (50  $\mu$ g) was incubated with <sup>225</sup>Ac at a labeling ratio of 1.85 MBq/ $\mu$ g for 45 min at 43°C, and chased with 1 mM DTPA. Radiolabeling efficiencies determined by instant thin layer chromatography were between 89-100% for all reactions.

## **Therapy**

Mice injected i.v. with MM1-S were randomized by BLI after 9-19 days, prior to the start of RIT. Mice were given IVIg by i.p. injection 2 hours prior to the start of radioimmunotherapy. For the high-dose  $^{177}\text{Lu}$  study, the mice were treated with saline, unlabeled Dara or 11.1 MBq  $^{177}\text{Lu}$ -DOTA-Dara. In a follow-up study, mice were treated with saline, 1.85, 3.7 or 7.4 MBq of  $^{177}\text{Lu}$ -DOTA-Dara. For  $^{225}\text{Ac}$  radioimmunotherapy, the mice were treated with saline, 22.2 kBq of untargeted  $^{225}\text{Ac}$ -DOTA-Tras, or 11.1 kBq or 22.2 kBq of targeted  $^{225}\text{Ac}$ -DOTA-Dara. For the lower-dose radioimmunotherapy study, the mice were treated with saline or 0.925, 1.85, or 3.7 kBq of untargeted  $^{225}\text{Ac}$ -DOTA-Tras, or 0.925, 1.85, or 3.7 kBq of targeted  $^{225}\text{Ac}$ -DOTA-Dara. All therapy doses were made up to 30  $\mu\text{g}$  antibody, for a total volume of 200  $\mu\text{L}$ .

## **Statistical Analysis**

ANOVA (Tukey's multiple comparison test) was used to analyze the tumor growth curves and log-rank Mantel-Cox test for survival curves, using Prism 7.02 (GraphPad Software). P-values for each group are reported as a measure of statistical significance compared to the vehicle control group. Differences were considered significant if  $p < 0.05$ .

## **Dosimetry and Mathematical Modeling Calculations.**

See Supplemental materials.

## RESULTS

### **<sup>177</sup>Lu-DOTA-Dara Radioimmunotherapy**

The anti-tumor activity of <sup>177</sup>Lu-DOTA-Dara was evaluated in a disseminated MM model using luciferase-transfected MM1-S cells injected i.v. in NSG mice, following cancer progression by bioluminescence (BLI). The mice were treated 19 days post MM1.S injection, at which point all mice showed disseminated MM by BLI. Weight loss was used as an appropriate measure of whole-body toxicity. While BLI measurements demonstrated that a dose of 11.1 MBq <sup>177</sup>Lu-DOTA-Dara caused significant regression of MM (Fig. 1A and B), there was little increase in median survival (36d) compared to the control groups (33d), likely indicating the mice died because of whole-body toxicity (Fig. 1C, Table 1, Supplemental Fig. 1). Because the 11.1 MBq dose had a minimal effect on survival, lower doses of <sup>177</sup>Lu-DOTA-Dara were investigated (Fig. 2, Supplemental Fig. 2). The 1.85 MBq group had an extended median survival of 44 days in contrast to 33d in the untreated control group (Fig. 2B) The median survival of the 3.7 MBq and 7.4 MBq groups was extended to 54d and 47d, respectively (Fig. 2B, Table 1). Because the median survival of the 7.4 MBq group was less than that of the 3.7 MBq group, the 7.4 MBq dose was the maximum tolerated dose. Notably, the control group exhibited substantial weight loss by day 30, because of MM burden (Figs. 1C and 2C). We thus found that  $\beta$ -emitter based RIT led to high toxicity, with a maximum increase of 60% in median survival in this model of disseminated MM.

### **<sup>225</sup>Ac-DOTA-Dara Radioimmunotherapy**

The  $\alpha$ -emitter <sup>225</sup>Ac was investigated with the hypothesis that there would be less off-target toxicity, because of its lower penetrative power, while still maintaining a therapeutic effect, due to its higher LET. A preliminary study was performed with two predicted high doses of <sup>225</sup>Ac-DOTA-Dara, 11.1 and 22.2 kBq, in the interest of defining whole-body toxicity. <sup>225</sup>Ac-DOTA-Trastuzumab was used as an untargeted control, since the MM1-S cell line is negative for HER2 expression (21). There was a dose-dependent reduction in the tumor growth curves, with targeted 22.2 kBq having the

highest impact on the delay of tumor regrowth as measured by whole-body BLI (Fig. 3A and B). The targeted 22.2 kBq group had almost double the median survival (64d) compared to untreated controls (33d), with an even greater improvement (77d) observed in the targeted 11.1 kBq group (Fig. 3B, Supplemental Fig. 3, Table 2). The lower median survival of the targeted 22.2 kBq group means that this group likely reached maximum tolerated dose, reflected by greater whole-body toxicity as measured by weight loss (Fig. 3C). The 22.2 kBq untargeted control group had an insignificant median survival of 36d compared to untreated controls and exhibited the highest level of whole-body toxicity (Table 2, Fig. 3C).

Targeted alpha therapy with lower doses of targeted  $^{225}\text{Ac}$ -DOTA-Dara compared to untargeted  $^{225}\text{Ac}$ -DOTA-Tras was performed to determine an optimal therapeutic effect while maintaining low whole-body toxicity. The untargeted control groups with doses of 0.925, 1.85 and 3.7 kBq showed an insignificant difference in median survival (35d) compared to the untreated control (33d) survival curves (Fig. 4, Supplemental Fig. 4, Table 2). Both the targeted 0.925 and 1.85 kBq dose groups had similar reduction in tumor growth, with a median survival of 45 and 52 days, respectively (Fig. 4B, Table 2). The targeted 3.7 kBq dose group showed the second highest therapeutic effect (72d), after the targeted 11.1 kBq dose (77d), more than doubling the median survival (Fig. 4B), while showing no significant difference in weight loss compared to the untreated controls (Fig. 4C).

### **Radiobiological Modeling**

The major differences in the results with  $\alpha$ - vs  $\beta$ -emitter radioimmunotherapy in disseminated MM was modeled in terms of differences between  $\alpha$ - and  $\beta$ -particle interactions with tissues that result in different cell survival characteristics. One would predict that, since the high LET radiation of  $\alpha$ -emitters deposit more energy per unit distance than  $\beta$ -emitters, they would affect more damage to the targeted cells. We quantified the radiobiological effects of the two radionuclides  $^{177}\text{Lu}$  and  $^{225}\text{Ac}$  with the Linear Quadratic model parameter  $\alpha(\text{Gy}^{-1})$ , which is associated with radiosensitivity. By fitting a mathematical model that accounts for MM proliferation and the action of the radioimmunotherapy to the tumor burden data, we observed a 10-fold increase in



radiation sensitivity of the MM tumors to  $^{225}\text{Ac}$ - compared to  $^{177}\text{Lu}$ -radioimmunotherapy for all tested doses, consistent with the relative biological effectiveness (RBE) of high LET alpha- compared to low LET beta-radiation (Fig. 5). Importantly, we observed a nonlinear relationship between radiosensitivity and injected dose activity for  $^{225}\text{Ac}$ , with a predicted peak of therapeutic radiosensitivity at a dose of 3.7 kBq (Fig. 5A). In contrast, much less variation in radiosensitivity was observed across dose levels for  $^{177}\text{Lu}$  (Fig. 5B). A table of model parameters and model parameter sensitivity analysis is provided in the supplemental material (Supplemental Figs. 5-6, Supplemental Table 1).

## DISCUSSION

Theranostics is a treatment strategy that combines diagnostics with therapy. Dara is a promising theranostic agent, since the antibody alone is FDA approved for MM therapy (22) and is being investigated as a carrier for the targeted delivery of cytotoxic agents (23). Caserta *et al.* showed that  $^{64}\text{Cu}$ -DOTA-Dara retained full immunoreactivity to CD38 and gave more specific and sensitive PET/CT tumor images than  $^{18}\text{F}$ fluoro-deoxyglucose (FDG) in a disseminated MM model (21). On the basis of the preclinical results,  $^{64}\text{Cu}$ -DOTA-Dara was approved for study in a clinical trial at City of Hope, in which imaging of MM patients also preliminarily showed higher sensitivity than that of the FDA-approved FDG imaging agent (24).

A recent study by Dawicki *et al.* used a similar  $^{225}\text{Ac}$ -DOTA-Dara construct for targeted alpha therapy in both lymphoma and MM mouse models (18). However, they used a subcutaneous (s.c.) xenograft model with therapy given via an intraperitoneal (i.p.) injection, versus the disseminated MM model used in our study, with the targeted alpha therapy given i.v. Whereas Dawicki *et al.* showed an anti-tumor effect with high doses of unlabeled Dara antibody alone, this result was not seen in our experiments, perhaps because of differences in immune status between the two mouse models. In the s.c. MM model, the researchers saw a decrease in tumor growth rate at a targeted alpha therapy dose of 14.8 kBq, and in our disseminated model targeted alpha therapy doses of 22.2 and 11.1 kBq prevented tumor progression up to 35 and 25 days post treatment, respectively. We believe that the disseminated MM model is more similar to the spread of MM in humans and that i.v. vs i.p. injections allow for more rapid systemic diffusion of the agent. Similarly to our study, Dawicki *et al.* observed no unacceptable toxicity in terms of weight loss. They also reported no significant difference in hematologic, liver or kidney toxicity between the targeted alpha therapy and control groups. Both studies indicate that the use of targeted alpha therapy to CD38 shows great promise in the treatment of MM, with little off-target toxicity.

Compared to targeted beta therapy, targeted alpha therapy caused a more pronounced regression of MM growth while displaying lower whole-body toxicity. As the total body absorbed dose increased, the median survival of  $^{177}\text{Lu}$  radioimmunotherapy

treated mice did not increase in a parallel fashion (Table 1), likely because of bone marrow toxicity, a consequence of the long path length of the  $^{177}\text{Lu}$   $\beta$ -emitter. In contrast,  $^{225}\text{Ac}$ -based targeted alpha therapy had less whole-body toxicity and displayed a dose-dependent therapeutic effect. As the total absorbed dose increased, the median survival also increased, a consequence of its lower path length and higher LET (Table 2). This effect is specific for targeted alpha therapy, since the untargeted alpha therapy led to no improvement in median survival with increasing doses. This effect was consistent with mathematical modeling, an approach that quantified the radiobiological effects of the radionuclides and predicted a maximal therapeutic radiosensitivity at 3.7 kBq of administered  $^{225}\text{Ac}$ -DOTA-Dara. Going forward, the 3.7 kBq dose of  $^{225}\text{Ac}$ -DOTA-Dara targeted alpha therapy shows the most promise, especially for combinatorial therapy, as its therapeutic efficacy is similar to the higher 11.1 and 22.2 kBq dose groups in causing initial regression of the MM and more than double median survival time, while not showing the significant toxicity seen with the higher-dose  $^{225}\text{Ac}$  groups. On the basis of our experience with targeted alpha therapy, it is likely that proper scaling of these doses to humans warrants evaluation in a clinical trial. Furthermore, in MM patients undergoing Dara therapy who experience tumor progression, Dara therapy is often discontinued, yet analysis of their cancer cells reveals continued CD38 expression (9,25). Thus, even previously treated Dara patients may be candidates for CD38 targeted alpha therapy.

Disclosure: Research reported in this publication was supported by the National Cancer Institute of the National Institutes of Health under grant numbers R01CA238429 (RR, JES, and FP), P30CA03357 (Cancer center support). 2. No other potential conflict of interest relevant to this article was reported.

## **KEY POINTS**

**QUESTION:** Can  $^{225}\text{Ac}$ -DOTA-Daratuzumab lead to a better tumor response and less whole-body toxicity compared to  $^{177}\text{Lu}$ -DOTA- Daratuzumab in a disseminated model of multiple myeloma?

**PERTINENT FINDINGS:** Targeted alpha therapy with  $^{225}\text{Ac}$ -DOTA-Daratuzumab at 3.7 kBq demonstrated optimal tumor response with no whole body toxicity, while  $^{177}\text{Lu}$ -DOTA- Daratuzumab showed no dose dependent tumor response and was toxic at all doses. Mathematical modeling of radiobiological effects demonstrated the superiority of targeted alpha therapy in a disseminated model of multiple myeloma.

**IMPLICATIONS FOR PATIENT CARE:** Targeted alpha therapy for disseminated multiple myeloma with proper scaling of  $^{225}\text{Ac}$ -DOTA-Daratuzumab doses to humans warrants evaluation in a clinical trial.

## REFERENCES

1. Siegel RL, Miller KD, Jemal A. Cancer statistics, 2019. *CA Cancer J Clin.* 2019;69:7-34.
2. Dimopoulos MA, Oriol A, Nahi H, et al. Daratumumab, Lenalidomide, and Dexamethasone for multiple myeloma. *N Engl J Med.* 2016;375:1319-1331.
3. Plesner T, Arkenau HT, Gimsing P, et al. Phase 1/2 study of daratumumab, lenalidomide, and dexamethasone for relapsed multiple myeloma. *Blood.* 2016;128:1821-1828.
4. Palumbo A, Chanan-Khan A, Weisel K, et al. Daratumumab, Bortezomib, and Dexamethasone for multiple myeloma. *N Engl J Med.* 2016;375:754-766.
5. Lokhorst HM, Plesner T, Laubach JP, et al. Targeting CD38 with daratumumab monotherapy in multiple myeloma. *N Engl J Med.* 2015;373:1207-1219.
6. Rajan AM, Kumar S. New investigational drugs with single-agent activity in multiple myeloma. *Blood Cancer J.* 2016;6:e451.
7. Phipps C, Chen Y, Gopalakrishnan S, Tan D. Daratumumab and its potential in the treatment of multiple myeloma: overview of the preclinical and clinical development. *Ther Adv Hematol.* 2015;6:120-127.
8. Pick M, Vainstein V, Goldschmidt N, et al. Daratumumab resistance is frequent in advanced-stage multiple myeloma patients irrespective of CD38 expression and is related to dismal prognosis. *Eur J Haematol.* 2018;100:494-501.
9. Viola D, Dona A, Caserta E, et al. Daratumumab induces mechanisms of immune activation through CD38+ NK cell targeting. *Leukemia.* 2020; epub ahead of print..
10. de Weers M, Tai YT, van der Veer MS, et al. Daratumumab, a novel therapeutic human CD38 monoclonal antibody, induces killing of multiple myeloma and other hematological tumors. *J Immunol.* 2011;186:1840-1848.
11. Viola D, Dona A, Gunes EG, et al. Immune mediated mechanisms of resistance to daratumumab. *Blood.* 2018;132:3201-3201.
12. Kang L, Jiang D, Ehlerding E, et al. Safety and dosimetry evaluation of radioimmunotherapy using <sup>177</sup>Lu-labeled antibodies in lymphoma. *J Nucl Med.* 2019;60:1004.

13. Visser OJ, Perk LR, Zijlstra JM, van Dongen GA, Huijgens PC, van de Loosdrecht AA. Radioimmunotherapy for indolent B-cell non-Hodgkin lymphoma in relapsed, refractory and transformed disease. *BioDrugs*. 2006;20:201-207.
14. Howell RW, Azure MT, Narra VR, Rao DV. Relative biological effectiveness of alpha-particle emitters in vivo at low doses. *Radiation research*. 1994;137:352-360.
15. Wild D, Frischknecht M, Zhang H, et al. Alpha- versus beta-particle radiopeptide therapy in a human prostate cancer model *Cancer Research*. 2011;71:1009-1018.
16. Quelven I, Monteil J, Sage M, et al. (212)Pb Alpha-Radioimmunotherapy targeting CD38 in multiple myeloma: a preclinical study. *J Nucl Med*. 2019;61:1058-1065.
17. Teiluf K, Seidl C, Blechert B, et al. alpha-Radioimmunotherapy with (2)(1)(3)Bi-anti-CD38 immunoconjugates is effective in a mouse model of human multiple myeloma. *Oncotarget*. 2015;6:4692-4703.
18. Dawicki W, Allen KJH, Jiao R, et al. Daratumumab-225Actinium conjugate demonstrates greatly enhanced antitumor activity against experimental multiple myeloma tumors. *Oncolimmunology*. 2019;8:1607673.
19. Xu XS, Dimopoulos MA, Sonneveld P, et al. Pharmacokinetics and exposure-response analyses of daratumumab in combination therapy regimens for patients with multiple myeloma. *Advances in therapy*. 2018;35:1859-1872.
20. Lewis MR, Raubitschek A, Shively JE. A facile, water-soluble method for modification of proteins with DOTA. Use of elevated temperature and optimized pH to achieve high specific activity and high chelate stability in radiolabeled immunoconjugates. *Bioconjug Chem*. 1994;5:565-576.
21. Caserta E, Chea J, Minnix M, et al. Copper 64-labeled daratumumab as a PET/CT imaging tracer for multiple myeloma. *Blood*. 2018;131:741-745.
22. McKeage K. Daratumumab: First Global Approval. *Drugs*. 2016;76:275-281.
23. Zhang X, Zhang C, Yang X, et al. Design, synthesis and evaluation of anti-CD38 antibody drug conjugate based on Daratumumab and maytansinoid. *Bioorg Med Chem*. 2019;27:479-482.
24. Copper 64Cu-DOTA-daratumumab positron emission tomography in diagnosing patients with relapsed multiple myeloma. <https://ClinicalTrials.gov/show/NCT03311828>.

**25.** Ghose J, Viola D, Terrazas C, et al. Daratumumab induces CD38 internalization and impairs myeloma cell adhesion. *Onc Immunology*. 2018;7:e1486948.

Table 1: Efficacy, toxicity, and whole body absorbed dose for <sup>177</sup>Lu radioimmunotherapy in MM1-S disseminated MM. The mean value of all mice in each condition is given except for survival, which is the median.

	<b>Vehicle Control</b> (n≤10) <sup>1</sup>	<b>Dara</b> (n≤4)	<b>1.85 MBq <sup>177</sup>Lu-DOTA-Dara</b> (n≤4)	<b>3.7 MBq <sup>177</sup>Lu-DOTA-Dara</b> (n≤5)	<b>7.4MBq <sup>177</sup>Lu-DOTA-Dara</b> (n≤5)	<b>11.1 MBq <sup>177</sup>Lu-DOTA-Dara</b> (n≤4)
<b>Duration of Tumor Growth Delay</b> (days post MM1-S inj.)	0	0	0	33	33	32
<b>Start of Weight Loss</b> (days post MM1-S inj.)	28 <sup>M</sup>	26 <sup>M</sup>	33 <sup>M</sup>	33 <sup>R</sup>	33 <sup>R</sup>	26 <sup>R</sup>
<b>Median Survival</b> (day post MM1-S injection)	33	31	44	54	47	36
<b>Whole Body Absorbed Dose</b> (Gray)	-	-	0.9	1.9	4.1	6.4

<sup>1</sup> Combined vehicle control groups from all the <sup>177</sup>Lu experiments.

<sup>M</sup> Weight loss due to multiple myeloma burden.

<sup>R</sup> Weight loss due to radioimmunotherapy toxicity.



Table 2: Efficacy, toxicity, and whole body absorbed dose for <sup>225</sup>Ac targeted alpha therapy in MM1-S disseminated MM. The mean value of all mice in each condition is given except for survival, which is the median.

	<b>Vehicle Control</b> (n≤16) <sup>1</sup>	<b>0.925 kBq <sup>225</sup>Ac-DOTA-Tras</b> (n≤6)	<b>1.85 kBq <sup>225</sup>Ac-DOTA-Tras</b> (n≤6)	<b>3.7 kBq <sup>225</sup>Ac-DOTA-Tras</b> (n≤6)	<b>22.2 kBq <sup>225</sup>Ac-DOTA-Tras</b> (n≤4)	<b>0.925 kBq <sup>225</sup>Ac-DOTA-Dara</b> (n≤6)	<b>1.85 kBq <sup>225</sup>Ac-DOTA-Dara</b> (n≤6)	<b>3.7 kBq <sup>225</sup>Ac-DOTA-Dara</b> (n≤6)	<b>11.1 kBq <sup>225</sup>Ac-DOTA-Dara</b> (n≤4)	<b>22.2 kBq <sup>225</sup>Ac-DOTA-Dara</b> (n≤4)
<b>Duration of Tumor Growth Delay</b> (days post MM1-S inj.)	0	0	0	0	0	16	16	29	36	43
<b>Start of Weight Loss</b> (days post MM1-S inj.)	22 <sup>M</sup>	22 <sup>M</sup>	22 <sup>M</sup>	22 <sup>M</sup>	0 <sup>R</sup>	39 <sup>M</sup>	39 <sup>M</sup>	73	0 <sup>R</sup>	0 <sup>R</sup>
<b>Median Survival</b> (days post MM1-S inj.)	33	35	35	35	36	45	51	72	77	64
<b>Whole Body Absorbed Dose</b> (Gray)	-	0.2	0.3	0.7	4.2	0.2	0.4	0.8	2.3	4.7

<sup>1</sup> Combined vehicle control groups from all the <sup>225</sup>Ac experiments.

<sup>M</sup> Weight loss due to multiple myeloma burden.

<sup>R</sup> Weight loss due to radioimmunotherapy toxicity.

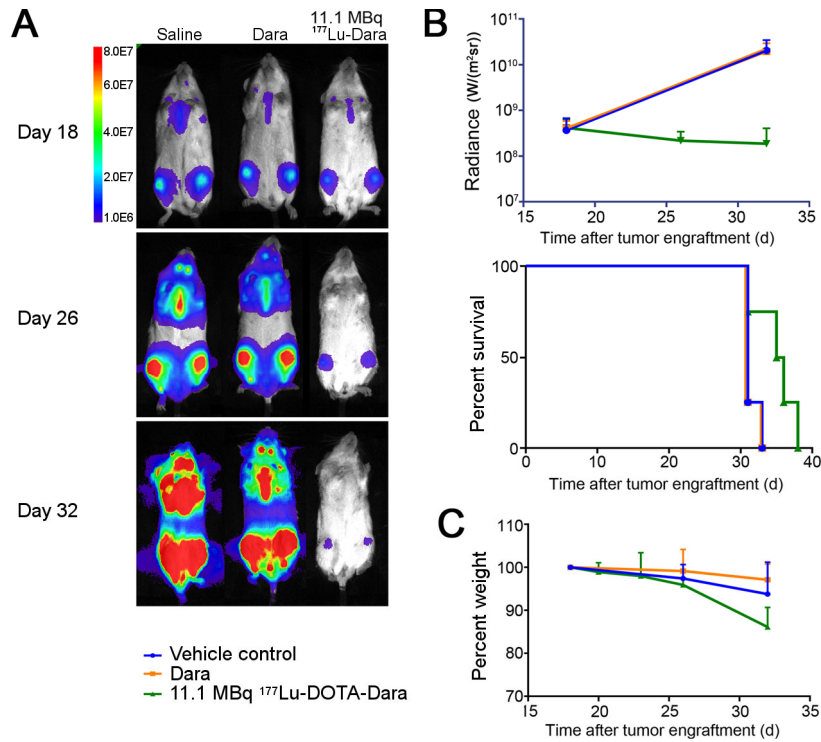


Figure 1: High dose <sup>177</sup>Lu-DOTA-Dara (11.1 MBq) for treatment of disseminated MM. (A) Representative bioluminescence images for each group, imaged weekly, intensity as indicated by color bar. A single mouse survived until day 36 (not shown in A). (B) Myeloma burden as quantification of the BLI images, in radiance: Dara ( $p > 0.999$ ), 11.1 MBq <sup>177</sup>Lu-DOTA-Dara ( $p = 0.038^*$ ); and Kaplan-Meier survival plot: Dara ( $p > 0.999$ ), 11.1 MBq <sup>177</sup>Lu-DOTA-Dara ( $p = 0.045^*$ ). (C) Whole-body toxicity as measured by weight. Dara ( $p = 0.883$ ), 11.1 MBq <sup>177</sup>Lu-DOTA-Dara ( $p = 0.914$ ).  $n = 4$  for all groups

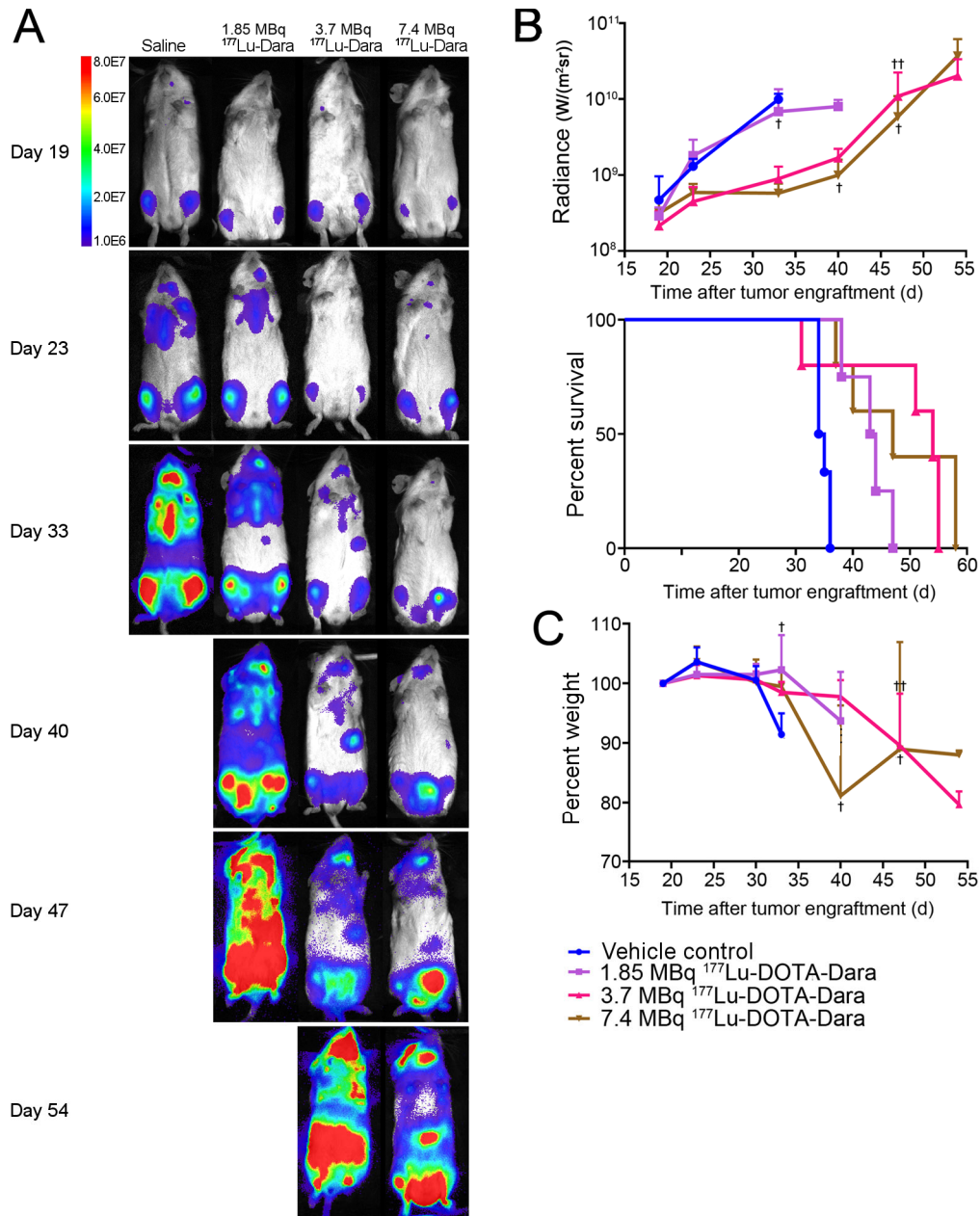


Figure 2: Dose response of <sup>177</sup>Lu-DOTA-Dara (1.85, 3.7, and 7.4 MBq) for treatment of disseminated MM model. (A) Representative BLI images for each group, intensity as indicated by color bar. (B) MM burden as quantification of the BLI images, in radiance: 1.85 MBq <sup>177</sup>Lu-DOTA-Dara (p=0.91), 3.7 MBq <sup>177</sup>Lu-DOTA-Dara (p=0.015\*), 7.4 MBq <sup>177</sup>Lu-DOTA-Dara (p=0.014\*); and Kaplan-Meier survival plot: 1.85 MBq dose (p<0.01\*\*), 3.7 MBq dose (p=0.0310\*), 7.4 MBq dose (p<0.01\*\*). Crosses indicate days on which mice were euthanized. (C) Whole-body toxicity as measured by weight. 1.85 MBq dose

( $p=.997$ ), 3.7 MBq dose ( $p=0.821$ ), and 7.4 MBq dose ( $p=.750$ ).  $n=6$  for saline group.  
 $n=4$  for 1.85 MBq group,  $n=5$  for 3.7 MBq and 7.4 MBq groups

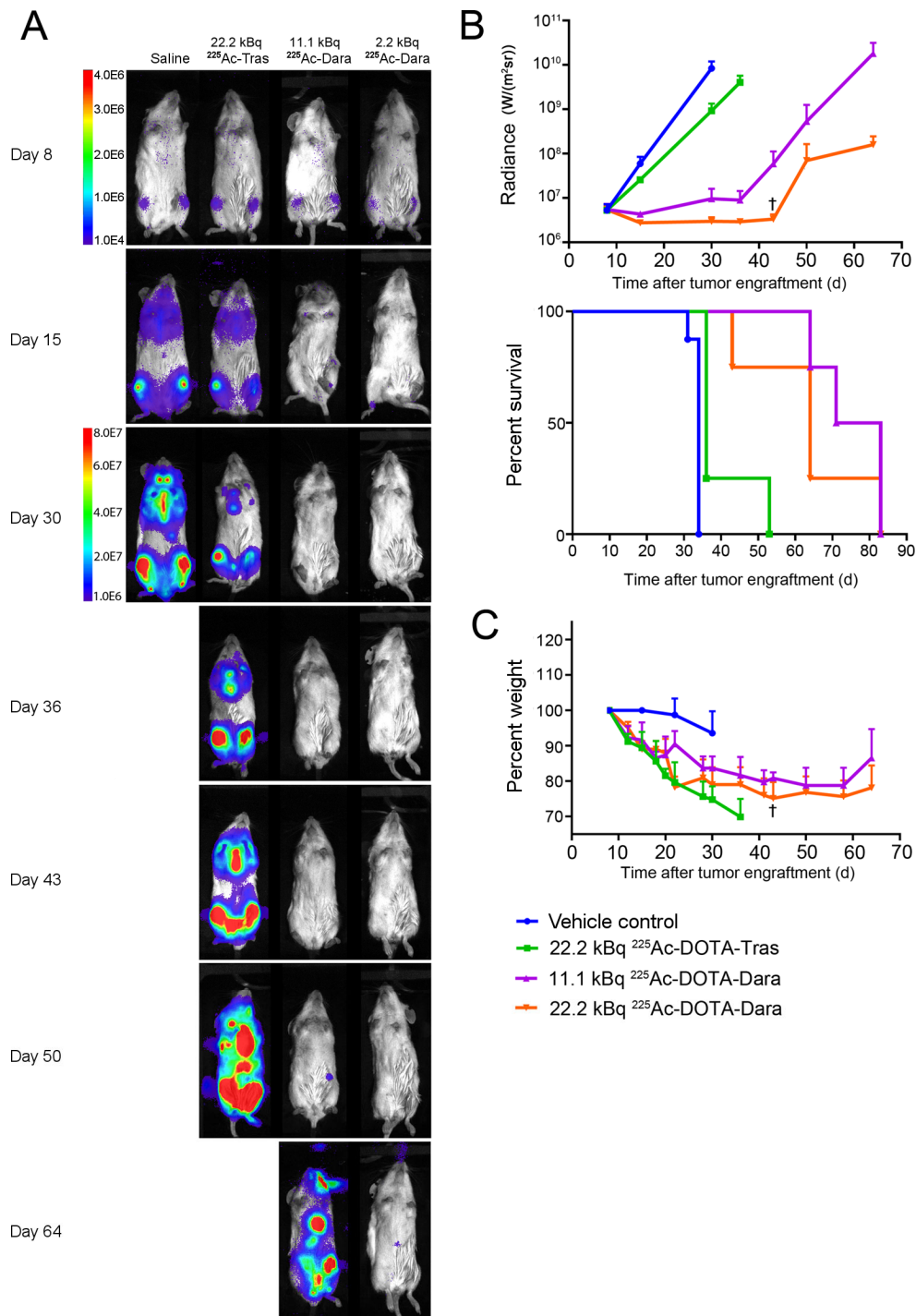


Figure 3: High dose of  $^{225}\text{Ac-DOTA-Dara}$  (11.1 and 22.2 kBq) for treatment of disseminated MM. (A) Representative BLI for each group, intensity as indicated by color bar. To visually compare groups >30d a separate scale was used. (B) MM burden based on quantification of the BLI in radiance: 22.2 kBq  $^{225}\text{Ac-DOTA-Tras}$  ( $p=0.035^*$ ), 11.1 kBq  $^{225}\text{Ac-DOTA-Dara}$  ( $p=0.015^*$ ), 22.2 kBq of  $^{225}\text{Ac-DOTA-Dara}$  ( $p=0.015^*$ ); and

Kaplan-Meier survival plot: 22.2 kBq  $^{225}\text{Ac}$ -DOTA-Tras ( $p < 0.01^{**}$ ), 11.1 kBq  $^{225}\text{Ac}$ -DOTA-Dara ( $p < 0.01^{**}$ ), 22.2 kBq  $^{225}\text{Ac}$ -DOTA-Dara ( $p < 0.01^{**}$ ). Crosses indicate days on which mice were euthanized. (C) Whole-body toxicity as measured by weight. 22.2 kBq  $^{225}\text{Ac}$ -DOTA-Tras ( $p = 0.0096^{**}$ ), 11.1 kBq  $^{225}\text{Ac}$ -DOTA-Dara ( $p = 0.0306^*$ ), 22.2 kBq  $^{225}\text{Ac}$ -DOTA-Dara ( $p = 0.0048^{**}$ ).  $n = 8$  for saline group,  $n = 4$  for treated groups.

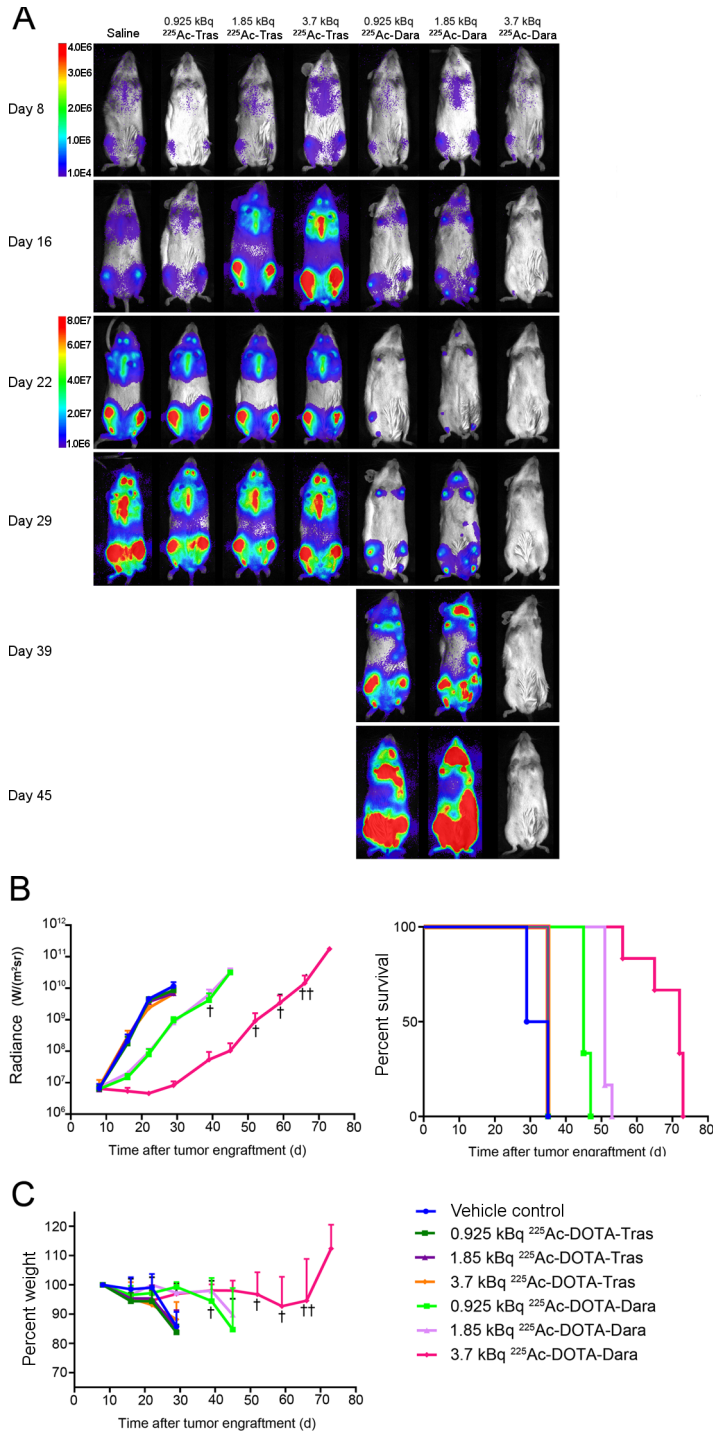


Figure 4: Dose response of <sup>225</sup>Ac-DOTA-Dara (0.925, 1.85, and 3.7 kBq) for treatment of disseminated MM. (A) Representative BLI for each group, intensity as indicated by color bar. After day 52 a single mouse survived until day 66 (not shown in A). To visually compare groups >30d a separate scale was used. (B) MM burden based on quantification of BLI in radiance: 0.925 kBq (p=0.96), 1.85 kBq (p=0.67) and 3.7 kBq

( $p=0.42$ )  $^{225}\text{Ac}$ -DOTA-Tras groups, 0.925 kBq ( $p<0.01^{**}$ ), 1.85 kBq ( $p<0.01^{**}$ ) and 3.7 kBq ( $p<0.01^{***}$ )  $^{225}\text{Ac}$ -DOTA-Dara groups; and Kaplan-Meier survival plot: 0.925 kBq ( $p=0.048^*$ ), 1.85 kBq ( $p=0.048^*$ ), and 3.7 kBq ( $p=0.048^*$ )  $^{225}\text{Ac}$ -DOTA-Tras groups, 0.925 kBq ( $p<0.01^{***}$ ), 1.85 kBq ( $p<0.01^{***}$ ), and 3.7 kBq ( $p<0.01^{***}$ )  $^{225}\text{Ac}$ -DOTA-Dara groups. Crosses indicate days on which mice were euthanized. (C) Whole body toxicity as measured by weight. 0.925 kBq ( $p=0.992$ ), 1.85 kBq ( $p=0.999$ ), and 3.7 kBq ( $p=0.999$ )  $^{225}\text{Ac}$ -DOTA-Tras groups, 0.925 kBq ( $p\geq 0.999$ ), 1.85 kBq ( $p\geq 0.999$ ), and 3.7 kBq ( $p=0.995$ )  $^{225}\text{Ac}$ -DOTA-Dara groups.  $n=8$  for saline group,  $n=6$  for therapy groups.



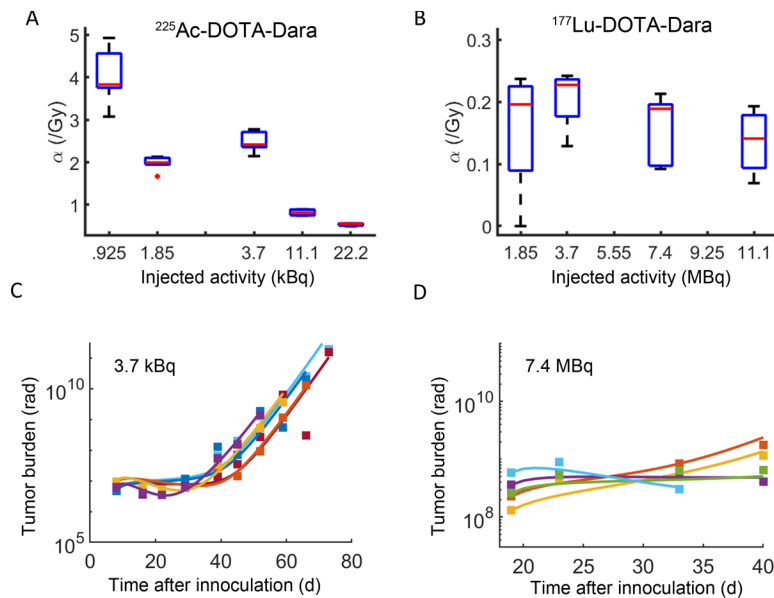


Figure 5: Radiobiological analysis of <sup>225</sup>Ac-DOTA-Dara and <sup>177</sup>Lu-DOTA-Dara therapy. Radiosensitivity parameter  $\alpha$  (Gy<sup>-1</sup>) is calculated for all dose levels of <sup>225</sup>Ac and <sup>177</sup>Lu DOTA-Dara treatments. (A) We observed a nonlinear relationship between radiosensitivity and dose for <sup>225</sup>Ac. Although 0.925 kBq results in the largest value of  $\alpha$ , this dose level did not confer a survival advantage. The model predicts 3.7 kBq of <sup>225</sup>Ac-DOTA-Dara to provide the largest radiosensitivity and therapeutic benefit relative to 1.85, 11.1, and 22.2 kBq doses. (B) Low LET <sup>177</sup>Lu results in 10-fold lower values of  $\alpha$  as compared to the high LET <sup>225</sup>Ac, and a less pronounced correlation with injected activity. (C,D) Tumor burden measured by bioluminescence over time and mathematical model fits for 3.7 kBq of <sup>225</sup>Ac and 7.4 MBq of <sup>177</sup>Lu, respectively. Note the difference in duration of response between <sup>225</sup>Ac and <sup>177</sup>Lu, 60-80 days versus 30-40 days.

## Comparison of CD38 targeted alpha- vs beta-radionuclide therapy of disseminated multiple myeloma in an animal model

Megan Minnix<sup>1,2\*</sup>, Vikram Adhikarla<sup>3\*</sup>, Enrico Caserta<sup>4\*</sup>, Erasmus Poku<sup>5</sup>, Russell Rockne<sup>3</sup>, John E. Shively<sup>1\*\*</sup> and Flavia Pichiorri<sup>4\*\*</sup>

### Supplemental Calculations and Figures

#### Dosimetry Calculation.

The decay in activity (disintegrations per second) for a radionuclide is given by the following equation:

$$A(t) = A_0 e^{-\lambda t} \quad (\text{Eqn S1})$$

where A is the activity at time t and A<sub>0</sub> is the initial activity of the radionuclide. The decay constant λ of the radionuclide and is related to the radionuclide half-life (t<sub>1/2</sub>) by  $\lambda = \frac{0.693}{t_{1/2}}$ . The total number of disintegrations (N) over a time interval from 0 to T is given by integrating the activity:

$$N = \int_0^T A(t) dt = \int_0^T A_0 e^{-\lambda t} dt = \frac{A_0}{\lambda} [1 - e^{-\lambda T}] \quad (\text{Eqn S2})$$

If the energy released per disintegration of the parent radionuclide is ε, the total energy (E) released in the duration T is given by

$$E = N\varepsilon = \frac{\varepsilon A_0}{\lambda} [1 - e^{-\lambda T}] \quad (\text{Eqn S3})$$

If the weight of mouse is given by W<sub>M</sub> (kg) the absorbed dose (Gy) in the mouse from the radionuclide is given by

$$D = \frac{E}{W_M} = \frac{\varepsilon A_0}{W_M \lambda} [1 - e^{-\lambda T}] \quad (\text{Eqn S4})$$

The average beta particle energy released from the decay of a single nucleus of <sup>177</sup>Lu is ε = 133 keV or 2.13 x 10<sup>-14</sup> J (1). The cumulative energy released from all alpha

particles emitted from a single disintegration of  $^{225}\text{Ac}$  and their daughter nuclei was calculated as  $\epsilon = 27.65 \text{ MeV}$  or  $4.42 \times 10^{-12} \text{ J}$ . The half-life of  $^{177}\text{Lu}$  is 6.7 days while the half-life of  $^{225}\text{Ac}$  is 10.0 days. Since the half-lives of the daughters of  $^{225}\text{Ac}$  are much shorter than 10.0 days they are ignored here for dosimetry purposes (2).

The absorbed dose was calculated for each mouse separately to account for their varying end points (T), and is reported as an average value per group. The absorbed doses for the following groups were calculated ( $^{177}\text{Lu}$  A<sub>0</sub>: 1.85 MBq, 3.7 MBq, 7.4 MBq, and 11.1 MBq;  $^{225}\text{Ac}$  A<sub>0</sub>: 0.925 kBq, 1.85 kBq, 3.7 kBq, 11.1 kBq, and 22.2 kBq). The initial weight of each mouse was used for  $W_M$ . Final average calculations for each group are shown in **Table 1**, for the  $^{177}\text{Lu}$  studies, and **Table 2**, for the  $^{225}\text{Ac}$  studies.

**Modeling Calculations.** To model the effect of  $^{177}\text{Lu}$  or  $^{225}\text{Ac}$  in inhibiting myeloma growth, we used a mathematical model with the guiding principle that it should be simple, with few free parameters and be parsimonious with the data. The model includes the proliferation of the tumor cells, the action of the radioimmunotherapy radiation, and the clearance of cells due to radiation-induced death. The most essential aspect of the model is the effect of the radiation due to the  $^{177}\text{Lu}$  or  $^{225}\text{Ac}$  radionuclide. We used the linear-quadratic (LQ) model for this purpose. The LQ is a standard model of tissue response to radiation, which relates the surviving fraction of cells,  $S$ , to radiation dose and is given by:

$$S(D) = e^{-\alpha D - \beta D^2} \quad (\text{Eqn S5})$$

where  $D$  is the radiation dose in units Gy (J/kg) and  $\alpha \text{ Gy}^{-1}$  and  $\beta \text{ (Gy}^{-2})$  are radiobiological constants corresponding to the linear and quadratic components of dose response respectively. To account for the decay rate of the radionuclide, we write the surviving fraction and dose as functions of time using a hazard ratio as:

$$\frac{dS(D(t))}{dt} = -h(t)S(D(t)) \quad (\text{Eqn S6})$$

where  $D(t)$  is the time-dependent dose to the tumor (3). The hazard function ( $h(t)$ ) is a rate constant with units  $\text{time}^{-1}$  and is given by the Lea-Catcheside dose protraction factor:

$$h(t) = \alpha R_0 e^{-\lambda_p t} + \frac{2\beta R_0^2}{\gamma - \lambda_p} (e^{-2\lambda_p t} - e^{-(\lambda_p + \gamma)t}) \quad (\text{Eqn S7})$$

where  $R_0$  is the initial dose rate in units Gy/time,  $\lambda_p$  is the decay constant ( $\text{time}^{-1}$ ) for the radionuclide and  $\gamma$  ( $\text{time}^{-1}$ ) is the cellular repair kinetics rate constant. The constants  $\alpha$  and  $\beta$  are the same as in the LQ model (Eqn S5).

To model the effect of a targeted radiation such as  $^{177}\text{Lu}$ - or  $^{225}\text{Ac}$ -DOTA-dara, we model two populations of tumor cells; unirradiated and irradiated (4,5). In this two compartment model, the first compartment ( $V_T$ ) represents tumor cells unexposed to radiation while the second compartment ( $V_R$ ) represents tumor cells exposed to radiation as follows:

$$\frac{dV_T}{dt} = \rho V_T - k_{Rx} V_T \quad (\text{Eqn S8})$$

$$k_{Rx} = \alpha R_0 e^{-\lambda_p t} + \frac{2\beta R_0^2}{\gamma - \lambda_p} (e^{-2\lambda_p t} - e^{-(\lambda_p + \gamma)t}) \gamma \lambda_p \quad (\text{Eqn S9})$$

$$\frac{dV_R}{dt} = k_{Rx} V_T - k_{cl} V_R \quad (\text{Eqn S10})$$

Unirradiated tumor growth is assumed to be exponential with growth rate constant  $\rho$ . Tumor cells in compartment  $V_T$  are irradiated and transferred to compartment  $V_R$  with the rate constant  $k_{Rx}$  given by the Lea-Catcheside equation (3). The irradiated tumor cells are cleared from the system at a rate  $k_{cl}$  ( $\text{time}^{-1}$ ) (**Supplemental Fig. 5**). The total tumor burden is given by the sum  $V = V_T + V_R$ . From equations S8-S10, the parameters  $\lambda_p, \gamma, R_0$  are fixed constants or determined by the treatment and the parameters  $\rho, \alpha, \beta, k_{cl}$  are free parameters. The tumor proliferation rate  $\rho$  is calculated by fitting exponential growth to the untreated control mice data. The mean proliferation rate from the controls was then used as a fixed parameter for the treated mice. The radiobiological parameters  $\alpha, \beta$  and the clearance rate constant  $k_{cl}$  are fit to the treatment data and used to quantify the effect of  $^{177}\text{Lu}$  and  $^{225}\text{Ac}$  therapy.

The radionuclides  $^{177}\text{Lu}$  and  $^{225}\text{Ac}$  have inherently different radiobiological characteristics due different radiation damage mechanisms.  $^{177}\text{Lu}$  produces beta particle emission while  $^{225}\text{Ac}$  produces in alpha particle emission. There are three beta

emissions from  $^{177}\text{Lu}$  nucleus that result in the majority of the dose delivered with an average energy of 133 keV with an average range of 0.23 mm in tissue, calculated using the continuous slowing down approximation model. The 5.8 MeV alpha particle emitted by  $^{225}\text{Ac}$  has a range of only  $\sim 60$   $\mu\text{m}$ , which is comparable to the diameter of a eukaryotic cell. The energy released from a cascade of alpha particles from decay of  $^{225}\text{Ac}$  and its daughters is 27.65 MeV. Due to the high energy transferred by an alpha particle over a short distance, alpha particles are classified as high Linear Energy Transfer (LET) radiation while beta particles are low LET. High LET alpha particle radiation has a larger relative biological effect as compared to a lower LET beta particles (6).

For mice treated with low LET  $^{177}\text{Lu}$ -DOTA-Dara, the radiobiological parameter ratio  $\alpha/\beta$  was held constant at 10 Gy. For high LET  $^{225}\text{Ac}$ -DOTA-dara, the radiobiological parameter  $\beta$  was set to zero. This results in the only free parameters in the mathematical model being  $\alpha$  and  $k_{cl}$ , which were calculated for each mouse. Parameters were optimized for  $^{177}\text{Lu}$ -DOTA-Dara and  $^{225}\text{Ac}$ -DOTA-dara cohorts separately by minimizing the least square residual for all dose levels simultaneously with *lsqcurvefit* in MATLAB (Mathworks, MA). The initial tumor burden at the start of therapy was taken as the initial condition for  $V_T$  and the initial number of irradiated tumor cells ( $V_R$ ) at  $t=0$  was zero.

In the mathematical model, the initial dose rate  $R_0$  ( $\text{Gy day}^{-1}$ ) was determined by the injected radioactivity. Given the injected activity, measured in Bq (disintegrations per second) and the decay characteristics of a particular radionuclide, the rate of energy emitted disintegration can be calculated. Thus, it is possible to calculate the amount of energy deposited in the tumor and thus the initial dose rate ( $R_0$ ) if the accumulated activity in the tumor and the mass of the tumor are known. An increase in the injected activity will result in a proportionate increase in the dose rate. However, since a measure of radioactivity in the tumor over time is unavailable, the initial dose rate and the injected activity ( $A_0$ ) were related by a proportionality constant  $\eta$  with units Gy/day/Bq as follows:

$$R_0 = \eta A_0 \quad (\text{Eqn S11})$$

The parameter  $\eta$  depends on the concentration of the radionuclide in the tumor. The constant  $\eta$  was taken as a unique global parameter and its value was determined by optimization.

### Calculation Parameters

*Proliferation rate  $\rho$* : The mean proliferation rate of control mice cohorts for each radionuclide was used as its proliferation rate.

*Radiosensitivity  $\alpha$* :  $\alpha$  was a free parameter optimized between literature-based limits (Table S1).

*Clearance rate  $k_{cl}$* :  $k_{cl}$  was free parameter optimized in the range 0 – 1 reflecting the limits of either having no clearance or 100% immediate clearance.

*Injected activity to initial dose rate conversion factor  $\eta$* : Mouse biodistribution studies indicated that the injected dose per gram varied between 3-60% ID/g (Data not shown) between mice. Assuming the injected activity is distributed uniformly within the mouse body, the following calculations were used to generate the limits for initial dose rates ( $R_0$ ) and thus  $\eta$ , for the radionuclides in the mathematical model. The average mouse weight is approximate  $W_M = 30$  g. The average activity concentration in the body is therefore given by  $C_M = \frac{100 \%ID}{30 \text{ g}} = 3.3 \frac{\%ID}{\text{g}}$ . The range of  $^{64}\text{Cu}$ -DOTA-Dara concentration in the tumor is estimated to be 3 – 60 %ID/g. Thus the ratio of tumor concentration to average body concentration ranges roughly from 1- 20. Assuming that the energy released due to a single decay of radionuclide to stable daughter is  $\mathcal{E}$  (J), then the energy released per second due to  $A_0$  Becquerels of activity is  $A_0 \times \mathcal{E}$  (J/s). If the activity is uniformly distributed in the mouse body, then the average dose rate in the mouse would be  $\dot{D}_{avg} = \frac{A_0 \mathcal{E}}{W_M}$ . However, if the activity is more concentrated in a region by a factor of  $f$ , then the dose rate in that region would be given by

$$\dot{D}_{tumor} = f \frac{A_0 \mathcal{E}}{W_M} \quad (\text{Eqn S12})$$

If, for instance, the biodistribution is measured via positron emission tomography, the factor  $f$  is the Standardized Uptake Value (SUV) of the radiotracer. This factor is seen to range between 1 and 20 as mentioned above from per the biodistribution data. Comparison with equation S11 for initial dose rate yields  $\eta = \frac{f\varepsilon}{W_M}$ . The energy released by beta particles from a single decay of  $^{177}\text{Lu}$  is 133 keV, and the energy released from a cascade of alpha particles from decay of  $^{225}\text{Ac}$  and its daughters is 27.65 MeV.

Converting this energy released to Joules the value of  $\eta$  calculated for  $^{177}\text{Lu}$  and  $^{225}\text{Ac}$  with  $f = 1$  are  $6.2 \times 10^{-8}$  and  $1.2 \times 10^{-5}$  Gy/day/Bq. With  $f$  varying between 1 and 20, the limits for  $\eta$  for  $^{177}\text{Lu}$  were taken to be  $6 \times 10^{-8}$  and  $1.1 \times 10^{-6}$  Gy/day/Bq, while the those for  $^{225}\text{Ac}$  were taken to be  $1.2 \times 10^{-5}$  to  $2.7 \times 10^{-4}$  Gy/day/Bq. The decay schemes of  $^{177}\text{Lu}$  and  $^{225}\text{Ac}$  are given by the Radioactive Decay Tables Handbook, U.S. Department of Energy November 1988.

We performed a sensitivity study of the model parameters (**Supplemental Table 1**) to evaluate the impact of parameters on the simulated tumor burden. As an example, the  $^{177}\text{Lu}$  data is used for this analysis. Each parameter is varied independently of the others to evaluate the effect of variations in that parameter on the predicted tumor burden (**Supplemental Fig. 6**). A smooth and continuous reduction in tumor burden with increased activity  $R_0$ , and radiosensitivity ( $\alpha$ ) is observed. Varying the tumor proliferation rate affects the rebound growth rate once the radionuclide has decayed and is no longer effective in controlling the tumor growth. Slower clearance of tumor cells from the irradiated compartment ( $V_R$ ) is indicated by lower clearance rate values, which result in increased tumor burden in the later stages once treatment fails. Clearance rate impacts the dynamics observed in the intermediate stage (day 1 - 40) of tumor growth and response to therapy. The result of this analysis is that the radiosensitivity and clearance rate constants have the most impact in shaping the tumor growth and response curves.

**Supplementary Table 1: Radiobiological model parameters**

Parameter	Symbol	<sup>177</sup> Lu		<sup>225</sup> Ac		References/ Comments
		Range	Initial Value	Range	Initial Value	
Tumor proliferation rate (days <sup>-1</sup> )	$\rho$	Constant (Control: 0.13 – 0.36)	0.26	Constant (Control: 0.32 – 0.42)	0.36	Range calculated for <sup>177</sup> Lu and <sup>225</sup> Ac groups separately and mean of each group used for further simulations
<i>Linear coefficient – radiosensitivity &amp; (Gy<sup>-1</sup>)</i>	$\alpha$	<i>0 - 0.4</i>	<i>0.05</i>	<i>0 - 5*</i>	<i>0.05</i>	van Leeuwen et al. Radiation Oncology (2018) 13:96 (7)
Radiosensitivity constants ratio (Gy)	$\alpha/\beta$	Constant	10	†	†	
<i>Clearance coefficient&amp; (day<sup>-1</sup>)</i>	$k_{cl}$	<i>0 – 1</i>		<i>0 – 1</i>	<i>0.1</i>	
Repair constant (day <sup>-1</sup> )	$\gamma$	Constant	16.6	-	-	Basic Clinical Radiobiology - Joiner (8)
Decay constant (day <sup>-1</sup> )	$\lambda_p$	Constant	0.103	Constant	0.1	
<i>Activity to dose conversion factor&amp; (Gy.day<sup>-1</sup>.<math>\mu</math>Ci<sup>-1</sup>)</i>	$\eta$	<i>Optimized in range 0.006 – 0.011</i>	<i>0.057</i>	<i>Optimized in range 1.2 – 27</i>	<i>9.43</i>	

\* $\alpha$  values for <sup>225</sup>Ac are much higher than for <sup>177</sup>Lu since the higher LET radiation has a higher relative biological effect (RBE). Typical values of RBE for alpha particles lie between 3 and 7.

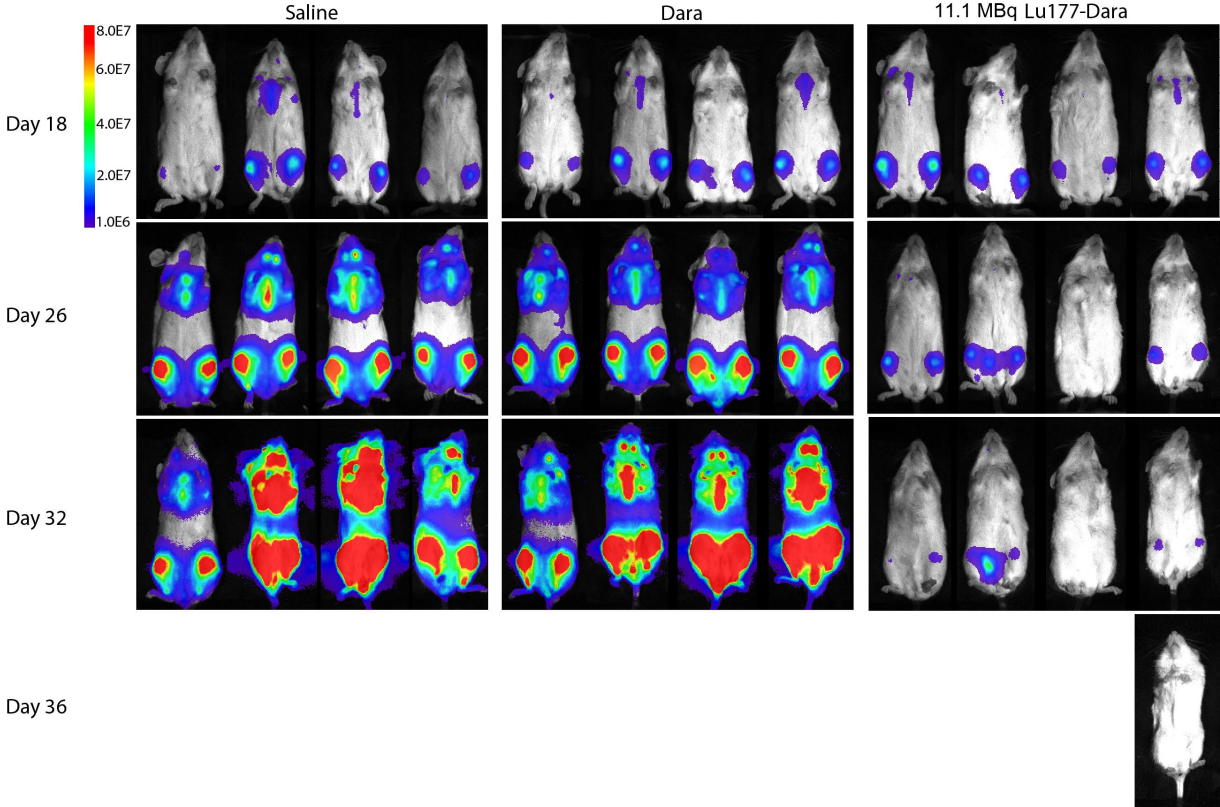
† The value of  $\alpha/\beta$  is undefined.

& Variables in italics are the parameters optimized in the simulations.

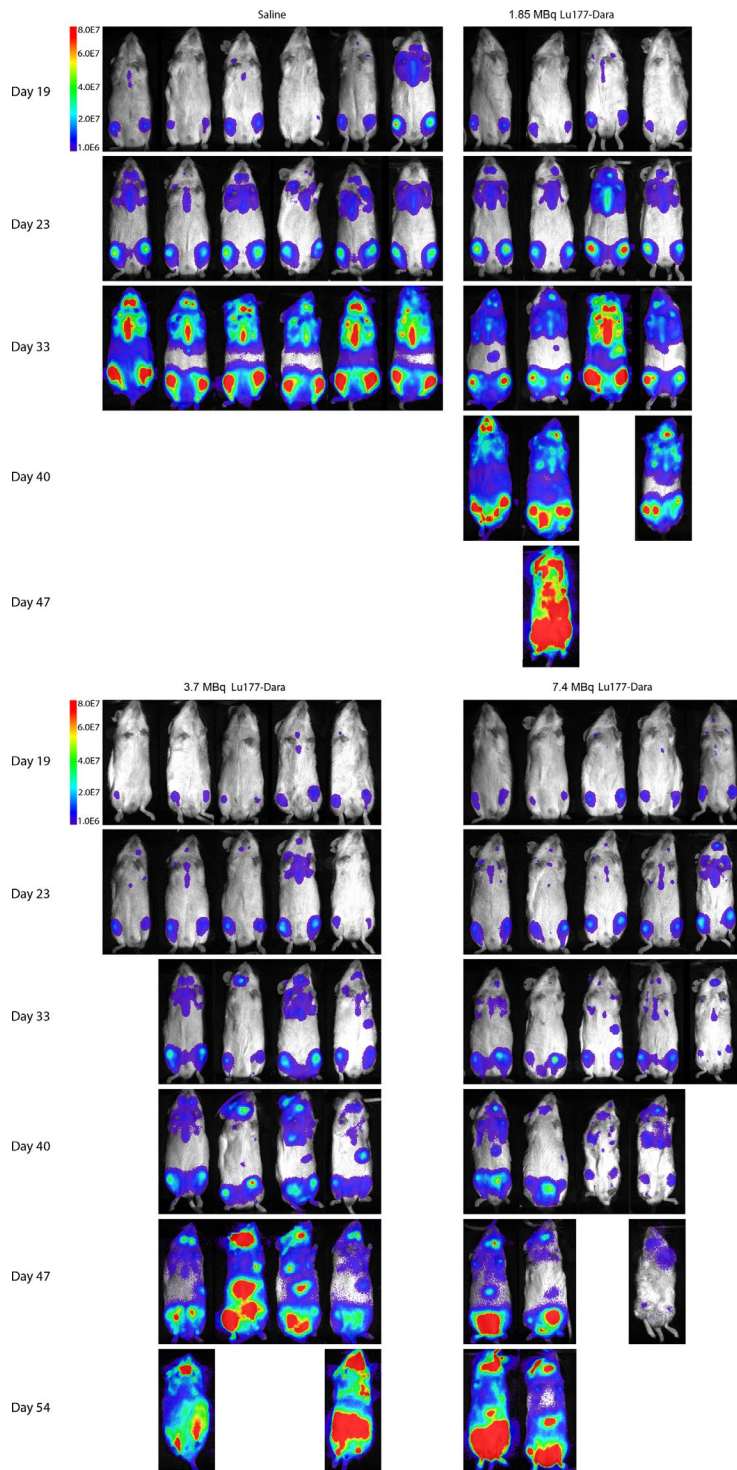


Supplemental Figures

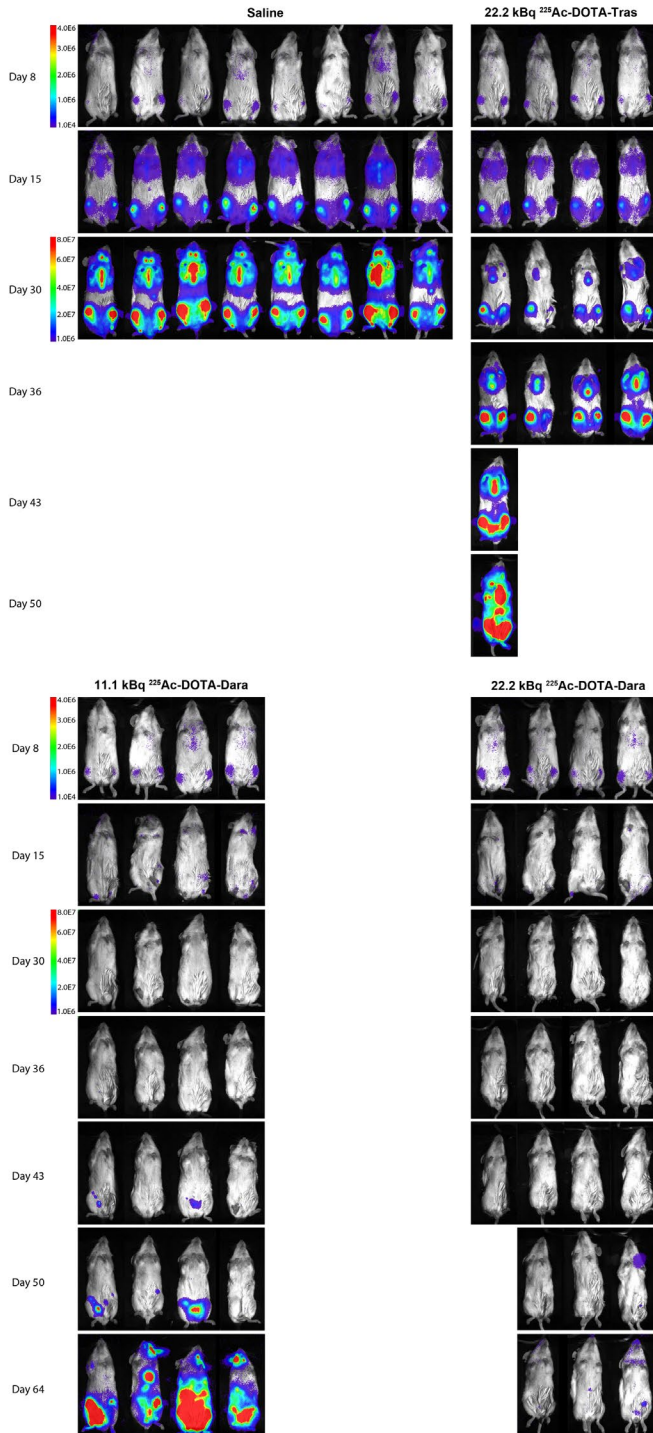
Supplementary Figure 1. High dose  $^{177}\text{Lu}$ -DOTA-Dara (11.1 MBq) for treatment of disseminated MM. Panels are of individual mice within each treatment group.



**Supplementary Figure 2. Dose response of  $^{177}\text{Lu}$ -DOTA-Dara (1.85, 3.7, and 7.4 MBq) for treatment of disseminated MM model. Panels are of individual mice within each treatment group.**



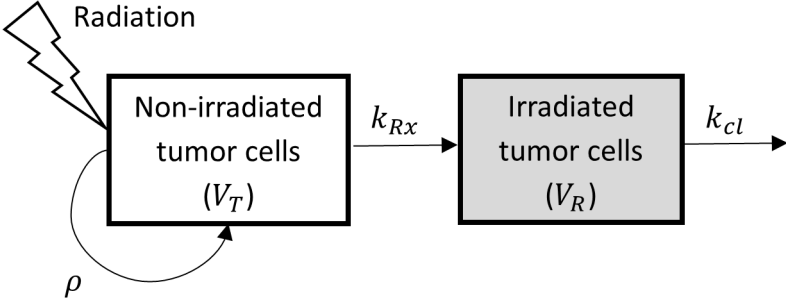
**Supplementary Figure 3. High dose of  $^{225}\text{Ac}$ -DOTA-Dara (11.1 and 22.2 kBq) for treatment of disseminated MM. Panels are of individual mice within each treatment group.**



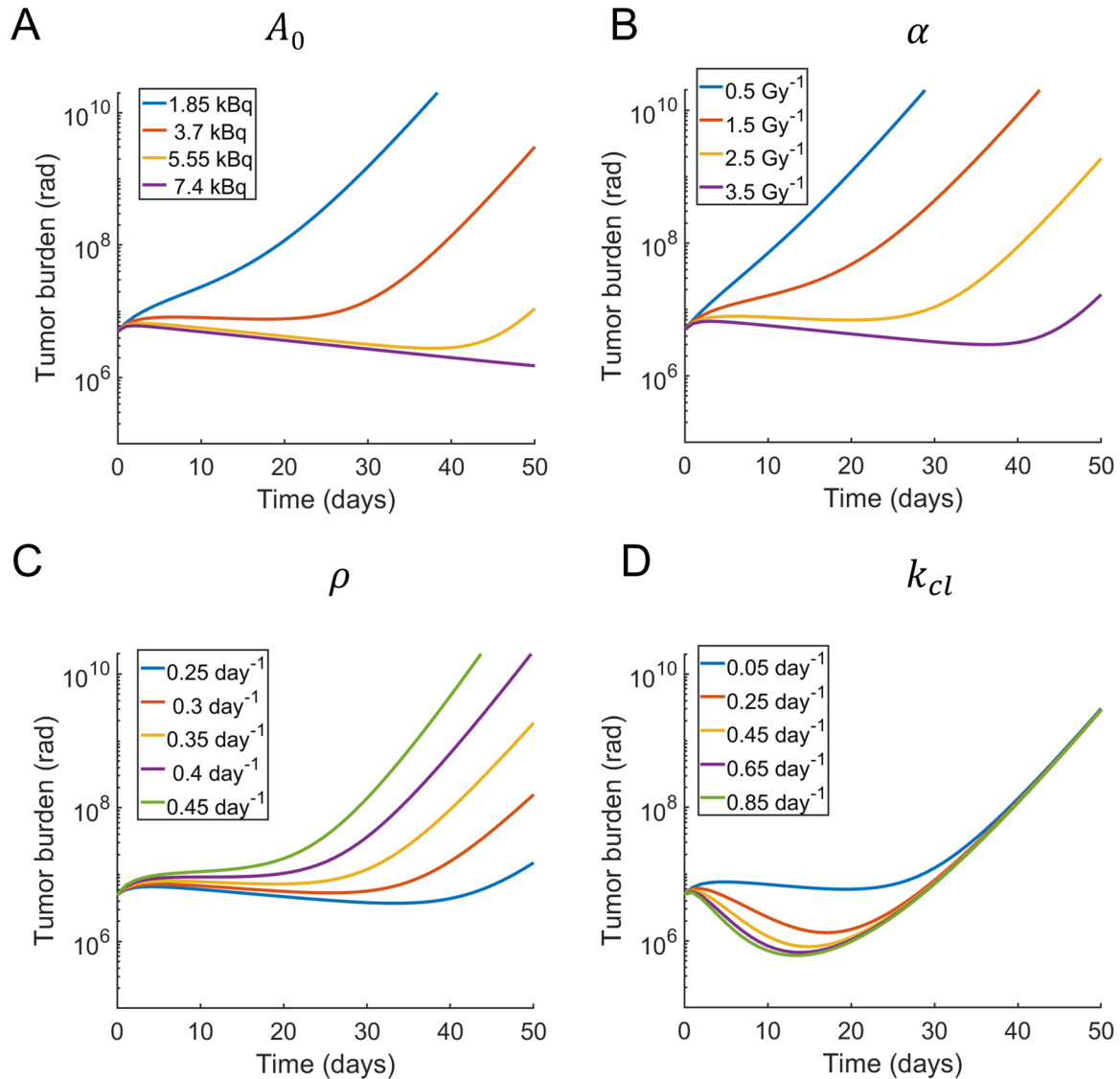
**Supplementary Figure 4. Dose response of  $^{225}\text{Ac}$ -DOTA-Dara (0.925, 1.85, and 3.7 kBq) for treatment of disseminated MM. Panels are of individual mice within each treatment group.**



**Supplementary Figure 5: Two-compartment mathematical model of CD38 targeted radio-immunotherapy.** Unirradiated myeloma tumor cells ( $V_T$ ) proliferate at a rate  $\rho$ , become irradiated ( $V_R$ ) at a rate  $k_{Rx}$ , and clear from the system at rate  $k_{cl}$ .



**Supplementary Figure 6: Sensitivity analysis.** Impact of model parameters on predicted tumor burden for  $^{225}\text{Ac}$ -DOTA-Daratumumab therapy. Each parameter is varied independently while the rest of the parameters were kept constant as a baseline set of parameters. (A) Injected activity ( $A_0$ ). (B) Radiosensitivity ( $\alpha \text{ Gy}^{-1}$ ). (C) Tumor proliferation rate ( $\rho$ ). (D) Tumor cell clearance rate from the irradiated tumor cells compartment ( $k_{cl}$ ). Baseline parameters used for the simulations:  $A_0 = 3.7 \text{ kBq}$ ,  $\alpha = 2.4 \text{ Gy}^{-1}$ ,  $\rho = 0.36 \text{ day}^{-1}$ ,  $k_{cl} = 0.03 \text{ day}^{-1}$



## **Supplementary References**

1. Koehler DC. *Radioactive decay data tables : a handbook of decay data for application to radiation dosimetry and radiological assessments*. [Oak Ridge, Tenn.]; Springfield, Va.: Technical Information Center, U.S. Dept. of Energy ; Available from National Technical Information Service, U.S. Dept. of Commerce; 1981.
2. Scheinberg DA, McDevitt MR. Actinium-225 in targeted alpha-particle therapeutic applications. *Current radiopharmaceuticals*. 2011;4:306-320.
3. Gong X. Maximal  $\varphi$ -inequalities for demimartingales. *Journal of Inequalities and Applications*. 2011;2011:59.
4. Sgouros G.  $\alpha$ -Particle–Emitter Radiopharmaceutical Therapy: Resistance Is Futile. *Cancer Research*. 2019;79:5479-5481.
5. O'Donoghue JA. The response of tumours with Gompertzian growth characteristics to fractionated radiotherapy. *International Journal of Radiation Biology*. 1997;72:325-339.
6. Goodhead DT. Mechanisms for the Biological Effectiveness of High-LET Radiations. *Journal of Radiation Research*. 1999;40:S1-S13.
7. van Leeuwen CM, Oei AL, Crezee J, et al. The alpha and beta of tumours: a review of parameters of the linear-quadratic model, derived from clinical radiotherapy studies. *Radiat Oncol*. 2018;13:96.
8. Joiner M, Kogel, A. van der *Basic Clinical Radiobiology*. 4th ed: Hodder Arnold; 2009.